

Document downloaded from:

<http://hdl.handle.net/10251/62079>

This paper must be cited as:

Roig Flores, M.; Serna Ros, P. (2015). Self-healing capability of concrete with crystalline admixtures in different environments. *Construction and Building Materials*. 86:1-11.
doi:10.1016/j.conbuildmat.2015.03.091.



The final publication is available at

<http://dx.doi.org/10.1016/j.conbuildmat.2015.03.091>

Copyright Elsevier

Additional Information

1 **Title:** Self-healing capability of concrete with crystalline admixtures in different environments

2 **Author names and affiliations:** M. Roig-Flores ^a (marroifl@upv.es), S. Moscato ^b (simone.moscato@gmail.com), P.
3 Serna ^a (pserna@cst.upv.es), L. Ferrara ^b (liberato.ferrara@polimi.it)

4 ^a ICITECH-Institute of Concrete Science and Technology, Universitat Politècnica de València, Valencia, Spain

5 ^b Politecnico di Milano, Milano, Italy

6 **Corresponding author:** M. Roig-Flores; marroifl@upv.es; Spain: +34 963877563 (Ext.:75631); ICITECH-Institute of
7 Concrete Science and Technology, Universitat Politècnica de València, 4N Building, Camino de Vera s/n, 46022
8 Valencia, Spain

9 **Present address:** M. Roig-Flores (marroifl@upv.es) ICITECH-Institute of Concrete Science and Technology,
10 Universitat Politècnica de València, 4N Building, Camí de Vera s/n, 46022 Valencia, Spain

11 **Abstract:** The aim of this study is analyzing the self-healing effect of a crystalline admixture in four types of
12 environmental exposure comparing with a reference concrete. Healing was studied by means of permeability tests on
13 cracked specimens and physical closing of the crack was observed by optic microscope and quantified through crack
14 geometrical parameters. The studied crack openings were under 300 µm and the time set for healing was 42 days. The
15 results show a different healing behavior depending on the exposure and the presence of the crystalline admixture,
16 demonstrating that the presence of water is necessary for the healing reactions.

17 **Keywords:** concrete, self-healing, autogenous, crystalline admixtures, permeability, durability

18 **1. Introduction**

19 Self-healing materials are those which have the capability of autonomously repairing small damages or cracks. The main
20 reason for investigating the properties of self-repairing materials is that constructions built with them will have increased
21 their service-life; likewise, structures with difficult or expensive reparations will benefit from self-healing their own
22 damages [1]. Thus, self-healing concrete will lead to an increase of the sustainability of the structures built with this
23 material.

24 Concrete has an inherent healing potential, called autogenous healing, which can take place in ordinary concrete elements
25 but its power is limited and is not predictable. Neville in 1981 already mentioned this phenomenon and proposed the
26 causes to autogenous healing [2]. He found out that fine cracks may heal completely under moist conditions and
27 explained this phenomenon by both the delayed hydration of unhydrated cement and carbonation. Later, those processes
28 were studied by Hearn (1998), Edvarsen (1999) and ter Heide (2005): all the authors agreed that the main processes
29 responsible of self-healing were delayed hydration for young concrete while carbonation was more relevant for older
30 elements [3][4][5]. Recent studies have compared the use of cement with different percentages of Portland cement and

31 additions in the autogenous healing process, obtaining better results with cements containing blast furnace slag or fly ash,
32 which enhance the effect of delayed hydration, while carbonation precipitation remains similar for the different binder
33 types [6][7][8]. Other studies were focused on the use of fibers in order to restrict crack width and enhance autogenous
34 healing [9][10], using different fibers made of different materials [11] and analyzing the healing process under different
35 environmental exposures [12].

36 In any case, autogenous healing is not a reliable phenomenon in order to get significant healing effects. That is the reason
37 why several new “engineered healing concepts” have been investigated in the last years, such as the use of
38 microencapsulated healing agents [13][14], bacterial concrete [15] or the use of crystalline admixtures [16].

39 Crystalline admixtures (CA) are a special type of permeability reducer admixtures (PRAs) as reported by the ACI
40 Committee 212 [17]. In contrast to water-repellent or hydrophobic products, these materials are hydrophilic, and this
41 makes them to react easily with water. When this reaction takes place, it forms water insoluble pore/crack blocking
42 deposits that increase the density of Calcium Silicate Hydrate (CSH) and the resistance to water penetration. In this case,
43 the matrix component which reacts is the tricalcium silicate (C_3S) and water presence is also needed. These products are
44 formed by active chemicals contained in cement and sand which form modified CSH, depending on the crystalline
45 promoter, and a precipitate formed from calcium and water molecules. Crystalline deposits become part of the matrix,
46 unlike hydrophobic materials, thus being able to resist pressures as high as 14 bars [17].

47 Some authors studied the visual closure produced by different additives in mortar specimens comparing with a reference
48 Portland mortar using fly ash, expansive admixtures, silica fume, crystalline admixtures and limestone powder with
49 complete water immersion as healing exposure [18]. It was shown that crystalline admixtures improved self-healing
50 processes at a higher rate than other types of additions, in the range of small cracks (less than 0.05 mm); however, they
51 became inefficient for wider cracks. In other studies, the self-healing measured by means of the evolution of the
52 permeability and visual closure was studied, comparing the effect of crystalline admixtures, expansive admixtures and a
53 combination of both products. The limits were shown of the self-healing capability of crystalline admixture for cracks
54 wider than 150 microns, while the combination of both agents achieved complete self-healing for cracks up to 400
55 microns after 30 days of water immersion [16]. Regarding to the recovery of mechanical properties, studying ordinary
56 concrete and high performance fiber-reinforced concrete with crystalline admixtures, a better self-healing response was
57 found for some parameters, such as the recovery of strength [19]. Other authors analyzed the healing effect of those
58 admixtures under four different exposures (water immersion with/without renovation, wet/dry cycles, humidity chamber
59 or air exposure) in terms of recovery of strength, obtaining the best results for the water immersion [19] or the wet/dry
60 exposure [20].

61 The study of self-healing properties is based on the controlled creation of a specific damage (e.g. cracks) and the
62 evolution of that damage under different conditions, which could be depicted by mechanical or durability properties. In
63 recent years different procedures have been published to this purpose. Several methodologies have been proposed in
64 order to analyze the permeability of cracked specimens, either simultaneously with the performance of load tests [21] or
65 using independent tests for each phase [16]. In regards to the relation between the induced damage and the permeability
66 properties, Edvardsen proposed a cubic relation between the water flow passing through a cracked concrete specimen and
67 the crack width with an expression derived from Poiseuille Law [4].

68 **2. Research objectives**

69 The main objectives of this research can be summarized as follows:

- 70 ▪ To analyze the effect of crystalline admixtures with reference to the enhancement of self-healing mechanisms.
- 71 ▪ To determine the influence of the environmental exposure in self-healing of concrete with and without
72 crystalline admixtures.
- 73 ▪ To develop and compare methods for evaluating the self-healing properties of cracked specimens, based on the
74 measure of the global permeability of the specimen and different geometrical characteristics of the crack before
75 and after the self-healing period.

76 **3. Experimental program and materials**

77 **3.1. Experimental program**

78 In this study, it was decided to maintain the crack width always under 0.3 mm, as it is a common threshold for crack
79 width in service state and it is potentially sealable by autogenous and CA healing, according to the available literature.
80 The age of pre-cracking was fixed at 2 days, as most of the cracks due to shrinkage may occur few days after casting
81 time. The initial permeability test was performed 1 day after pre-cracking, because of the needs related to the
82 experimental procedure. Finally the time set for the self-healing process before the last permeability evaluation was 42
83 days; as a matter of fact, in most studies specimens got sealed in a smaller period of time when exposed to water
84 immersion.

85 The experimental variables which were studied in this research are:

- 86 ▪ Crystalline admixture dosage: 0% (control specimens), 4% by the weight of cement (CA specimens).
- 87 ▪ Self-healing exposure: water immersion (WI), water contact (WC), humidity chamber (HC) and air exposure at
88 laboratory conditions (AE)

89 This study includes both, a main study of permeability evolution and an analysis about the methodology for image
90 evaluation of the crack. A total of eight groups of specimens were cast for permeability tests, each consisting of six

91 concrete specimens. Additional specimens were cast for some groups that required further exploration. Among all the
 92 specimens: three per each group were also employed for image evolution of crack parameters. An overview of the final
 93 number of cast specimens for each group is summarized in Table 1: as a whole 61 specimens were tested for permeability
 94 whereas image analysis of the cracks was performed on 24 specimens.

Concrete	Exposure conditions	Number of specimens for permeability tests	Number of specimens for image analysis tests
Control	Water Immersion	6	3
	Water Contact	7	3
	Humidity Chamber	8	3
	Laboratory Conditions	9	3
CA	Water Immersion	8	3
	Water Contact	8	3
	Humidity Chamber	8	3
	Laboratory Conditions	7	3

95 **Table 1. Number of specimens cast for each group**

96 3.2. Materials and mixture proportions

97 It was decided in this study to work with fiber-reinforced concrete. Since the focus of the project was to study the healing
 98 effects on pre-cracked specimens, fibers could provide an effective action both in controlling crack width during the pre-
 99 cracking process as well as in keeping fixed its value afterwards. The quantity of steel fiber was fixed at 40 kg/m³
 100 according to the criterion of making the crack opening easily controllable while avoiding excessive branching of cracks.

101 The cement used was CEM II/A-L 42.5 R from Elite Cementos S. L. The water/cement ratio used was 0.45 in both types
 102 of concrete. A dosage of 4% by the weight of cement of crystalline admixture in powder form was introduced in the CA
 103 Concrete whose behavior was compared with control specimens (without crystalline admixture). The two mix designs are
 104 shown in Table 2.

105 The criterion chosen for making concrete mixes with and without crystalline admixture is to maintain constant the sum of
 106 limestone powder and crystalline admixture, due to their similar effect on concrete workability. As a matter of fact they
 107 would both act as densifiers of the paste matrix phase. Superplasticizer, ViscoCrete 5720, dosage was adjusted in each
 108 different group in order to get similar slump (140 mm ± 20 mm).

109 In total, 7 batches of control concrete and 6 of crystalline admixture concrete were cast. For each batch, three Φ150 x 300
 110 mm cylindrical specimens were cast according to UNE-EN 12390-2 to determine the compressive strength at 28 days, as

111 per UNE EN 12390-3. All batches were also characterized by their workability with slump test as per UNE EN 12350-
 112 2:2009. These control tests were performed with the objective of verifying the homogeneity of specimens of different
 113 batches but belonging to a same mix group (either control or CA) and in order to compare the results between the two
 114 mix groups (control and CA). After averaging the results of all batches for each group, it was observed that CA concrete
 115 had a significantly better compressive strength, about 15% higher than control concrete. With reference to the slump test
 116 results, differences are slightly lower, since the average results are around 13 cm for control concrete and 15 cm for CA
 117 concrete, which are within the acceptable tolerance limits of slump tests according to the standards.

Material (kg/m ³)	Control	CA Concrete
Cement II/A-L 42.5 R	350	350
Water	157.5	157.5
Gravel (4-12 mm)	950	959
Natural sand	899	875
Fibers, Dramix 65/35	40	40
Limestone powder	50	36
Crystalline Admixture	-	14
Average Slump (cm)	13	15
Average Compressive Strength (MPa)	53	61

118 **Table 2 - Mix design of control and CA concrete**

119 **4. Experimental methodology**

120 The methodology used in this research to evaluate the effects of self-healing consists of four stages: first, the creation of
 121 controlled damage in the specimens; second, the measure of the recovery of certain properties, such as permeability or
 122 crack geometrical parameters; third, the simulation of the conditions or environmental exposure needed to achieve better
 123 healing results and, finally, the evaluation of the recovery of the same property measured in the second stage.

124 **4.1. Creation of a damage: pre-cracking process**

125 Each cylindrical specimen with dimensions of $\Phi 150 \times 300$ mm was cut in half using a circular saw for concrete. In this
 126 way, the specimens' size for the permeability test was $\Phi 150 \times 150$ mm. The edge faces of each $\Phi 150 \times 150$ mm cylinder
 127 were then polished in order to eliminate mortar layers (in the bottom surface in contact with the moulds) and asperities
 128 (in the top free surface of the specimen as cast).

129 The specimens were pre-cracked at the age of 2 days, inducing, by means of a splitting test, a controlled damage (Figure
 130 1): this was meant as the width of the diameter crack, which was set to reach a target value, controlled by a calibration

131 ruler. The measure of the crack width with the calibration ruler while performing the splitting test has been meant as
132 good enough for the purpose of the campaign. As a matter of fact, though it is an approximate way to measure the crack
133 width, it is also very simple and allows a larger amount of specimens to be cracked in a reasonable time. The calibration
134 ruler has an inherent dispersion due to the human factor. Nevertheless it is a good method to obtain crack widths within a
135 range of 0-0.3 mm. If higher precision is needed, however, other methodologies to control the crack width during the
136 splitting test should be used.



137

138

Figure 1 - Pre-cracking process of a concrete specimen

139 Once cracked, specimens were kept in the healing exposure to let the self-healing agent to act for a specified period of
140 time. The self-healing effect has been checked by analyzing the concrete permeability of cracked specimens before and
141 after the self-healing process and with the evolution of geometrical parameters of cracks, namely its width and/or area.

142 **4.2. Evaluation of properties: permeability test**

143 A method based on the permeability test described in UNE-EN 12390-8 was employed in this study, but measuring the
144 water flow instead of the water depth penetration. To guarantee the impermeability of the specimen lateral surface, the
145 zones of the lateral surface which were in contact with the machine loading platens during the pre-crack splitting tests
146 were sealed with an epoxy resin Sikadur 31-CF as shown in Figure 2. It should be noted that resin does not enter
147 significantly inside the crack, since it is only placed externally.

148

149

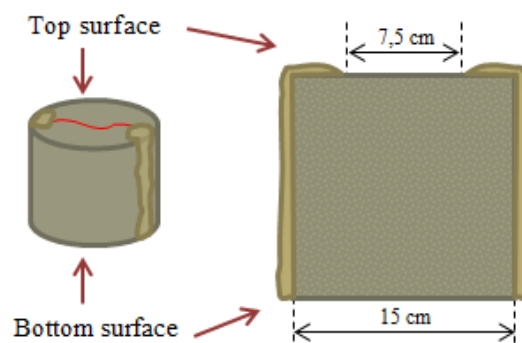
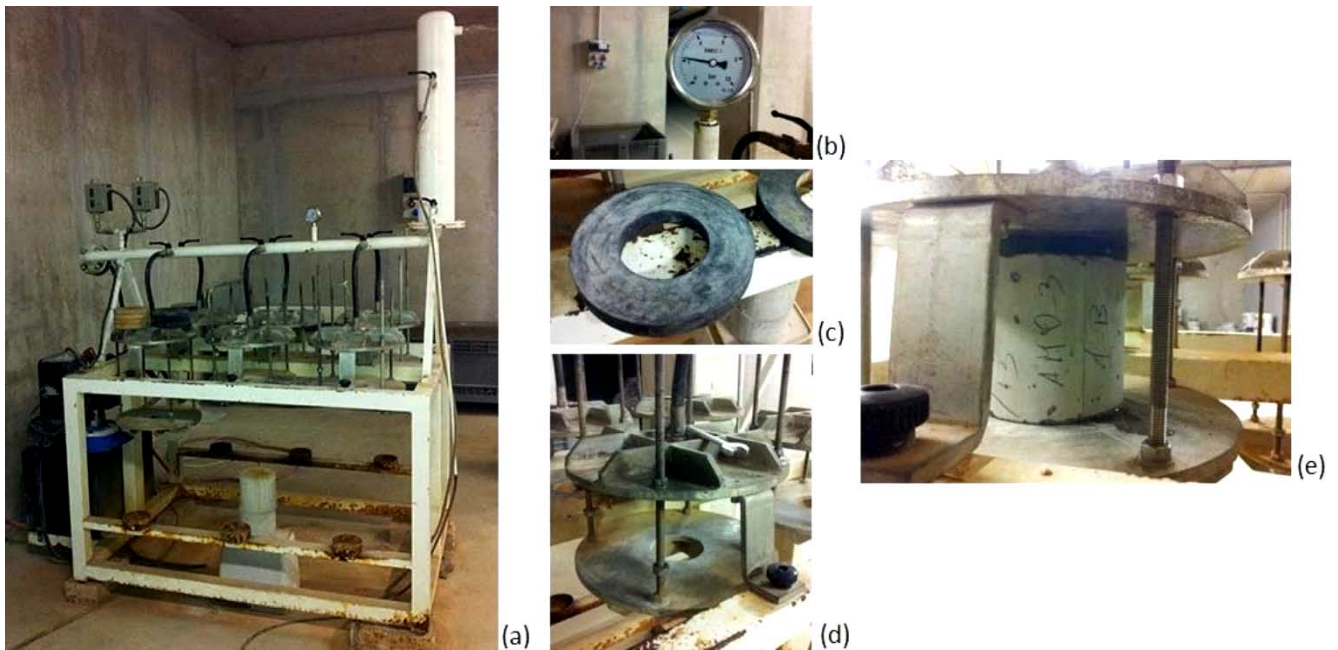


Figure 2 - Lateral sealing of specimens with Sikadur

150 The test was performed by applying a head water pressure equal to 2.00 bars. In practice, the initial pressure is set equal
151 to 2.05 bars and as pressure decreases due to water flow, the permeabilimeter turns on again when a pressure of 1.95 bars
152 is reached, recovering the 2.05 bars pressure. Therefore, water pressure is always kept between 1.95 and 2.05 bars. The
153 quantity of water passing through the crack was measured during a 5 minutes testing time. This procedure results in
154 higher water flows for larger crack widths. In this way, if a crack closes after the healing process, the water flow should
155 have been diminished. The permeabilimeter used in the test and the different parts it consists of it are shown in Figure 3.



156

157 **Figure 3 - Permeabilimeter (a) and its parts: manometer (b), sealing ring (c), auxiliary structure (d), prepared**
158 **specimen (e)**

159 4.3. Evaluation of properties: study of crack geometrical parameters

160 In addition, crack geometry parameters (width and area) were also measured to support measurements from permeability
161 tests. The crack width/area measurements are based on the study of composed panorama pictures showing the cracks all
162 along their length; the photography software Adobe Photoshop CS6 was used for image processing. The pictures were
163 taken before and after the healing exposure, with a digital optical microscope (x60, x200). Before taking pictures all the
164 specimens were cleaned with compressed air.

165 This method is more precise and reliable than the measurements which can be obtained by using the transparent
166 calibration ruler since through the use of the graphical software is possible to choose the real width bypassing the error
167 related to the human eye, which in smaller cracks, as those studied in this research, becomes more relevant.

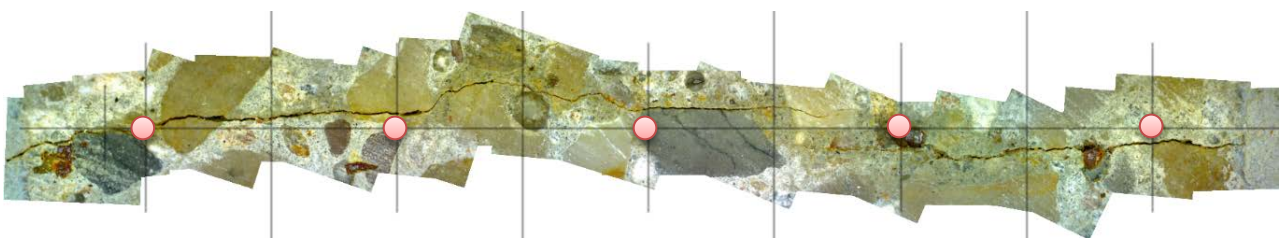
168 The measurement of crack geometrical parameter has been performed with a twofold purpose: first, to seek a correlation
169 with the water flow measured in the permeability tests; and, second, to analyze the significance of the evolution of the

170 same geometrical parameters as indicators of self-healing. To this twofold purpose, the ratios between final and initial
171 values of the water flow and of crack geometrical parameters were calculated. Water permeability is considered the
172 reference value in order to compare the different methods for quantifying self-healing, since the main objective of closing
173 a crack is to avoid the entrance of liquids, contaminants and aggressive agents.

174 Crack geometrical parameters can be divided in two groups: the measure of crack width and the measure of crack area.
175 The measure of crack width is the most used method to analyze geometrical evolution of cracks, because of its simplicity.
176 However crack area was expected to be a better indicator of the physical closing, because it would include the crack
177 width all along the whole length of the crack. Four crack geometrical parameters were measured in this paper:

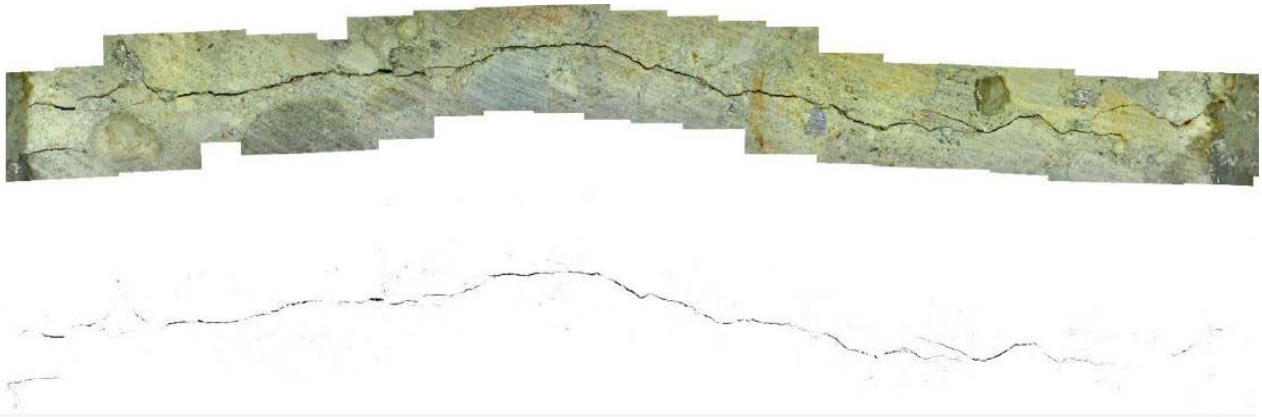
- 178 ▪ Two measures of crack width:
 - 179 ▪ w_{max} , maximum crack width: by means of graphic software, the maximum crack width is determined in
180 millimeters.
 - 181 ▪ w_{avg} , average crack width: by means of graphic software, crack width (in millimeters) is determined in
182 five fixed positions and averaged.
- 183 ▪ Two measures of crack area:
 - 184 ▪ A_{est} , estimated from average crack width w_{avg} : using the five measures of crack width and multiplying
185 by their associated lengths, in squared millimeters.
 - 186 ▪ A_{px} , measuring black pixels: by using graphic software, black pixels in the image are counted, which
187 indicate crack area.

188 With reference to the measure of the crack width, the maximum width w_{max} was calculated searching the highest value of
189 width all along the whole crack length in the high-resolution panoramas. For instance, the average width w_{avg} was
190 calculated averaging five width measurements, taken at prescribed positions along the crack, thus decreasing the
191 uncertainty of the measurement itself. A grid was prepared to overlap on the panorama pictures, after bringing the grid at
192 the same scale of the picture (Figure 4). Precisely, two grids were used, one for the top cracks and the other for the
193 bottom cracks, because of the different crack length in each surface (7.5 cm in the top crack and 15 cm in the bottom).



194
195 **Figure 4 - Panorama of a top crack and grid marking the measuring points**

196 The second group consists of the measurement of an averaged crack area and the measure of black pixels in an image. By
197 means of the same approach used to calculate w_{avg} , the area of the cracks is estimated by multiplying the five measured
198 widths, in millimeters, by their associated lengths obtaining the area in squared millimeters A_{est} . In this way, the resulting
199 area is approximated as the sum of the areas of five rectangles. The second method to calculate the area of the cracks
200 involves the use of the graphical software to quantify the number of black pixels inside the pictures. The basic concept is
201 that the cracks are shown as a black area, thus a higher number of black pixels corresponds to a greater area of the crack.
202 In order to avoid that pores or other dark parts of the pictures affect the quantification of black pixels, all the panoramas
203 were cleaned by a specific tool of the software (Figure 5).



204
205
206 **Figure 5 - Panorama of a top crack and its black pixels (before cleaning).**

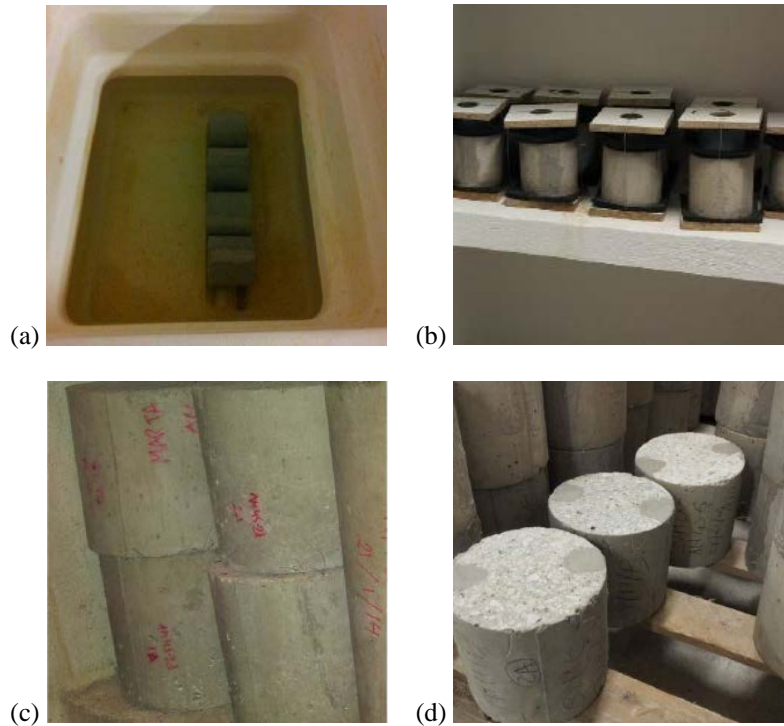
207 Each specimen has got two cracks (top and bottom), denoted according to the orientation of the same specimen in the
208 permeability test, and the water contact exposure. The relationship between water flow and the geometrical crack
209 parameters was studied. In this case, it is expected that a wider crack parameter leads to a bigger water flow result. It has
210 been studied if the geometrical crack parameter that should be considered is the value corresponding to: the top/bottom
211 crack, the maximum/minimum crack or the average of the two cracks.

212 **4.4. Exposure simulation**

213 Four environmental exposures were studied in order to determine the effect of humidity on the self-healing capability of
214 the tested specimens, comparing the reference concrete with the crystalline admixture concrete (Figure 6).

- 215 a. WI (Water immersion): continuous immersion in tap water at laboratory conditions without renewing the water
216 during the healing period (temperature of water, 15-16°C)
- 217 b. WC (Water contact): a layer of water with a head pressure of 2 cm-water on the top crack, and storage in
218 humidity chamber at 20°C and 95±5% relative humidity. Additional water was supplied when necessary in order
219 to maintain the 2 cm water layer.

- 220 c. HC (Humidity chamber): storage of the specimens inside a standard humidity chamber at 20°C and 95±5%
221 relative humidity.
- 222 d. AE (Air Exposure): storage of the specimens in normal laboratory conditions inside a room without exterior
223 influences.

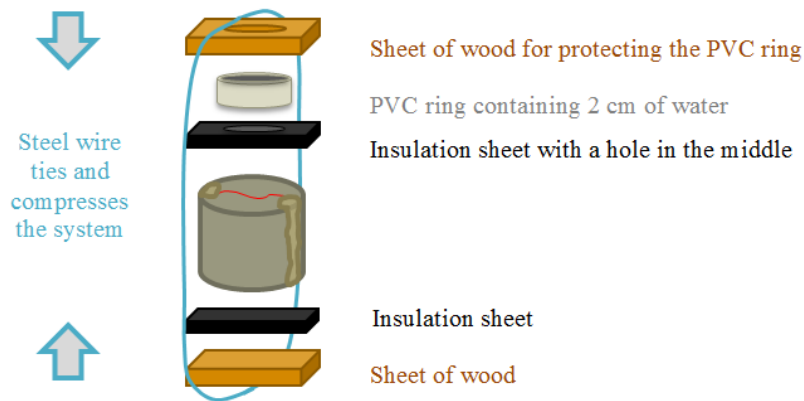


224 **Figure 6 - Four exposures: water immersion (a), water contact (b), humidity chamber (c) and air exposure (d)**

225 Each type of healing exposure has been designed with the objective of simulating real conditions. WI simulates
226 underwater concrete elements; WC simulates situations with a face directly exposed to water with a very low pressure
227 and the other unexposed to it, such as buried walls under the water table; HC simulates concrete elements without direct
228 contact with water but constructed in a high humidity environment and AE concrete elements without direct contact with
229 water and average humidity levels. With these four environmental conditions, it is intended to discern if the self-healing
230 will be powerful enough for constructions in several types of environments as above, including those without direct
231 contact with water and those elements in contact with it, either having a small amount of water in contact or totally
232 immersed.

233 The specimens immersed in water during the healing period, were divided in two different water recipients, in order to
234 avoid interferences between control concrete and concrete with crystalline admixtures. The immersed specimens were
235 placed on two 3 cm wide wood strips ensuring a separation between specimens of at least 5 cm between the cracked faces
236 and 1 cm between the lateral surfaces, in order to let the water act in the whole specimen.

237 The setup for the 2 centimeters water contact environment is shown in Figure 7. In this group, water remains in the upper
238 PVC ring and enters inside the specimen through the crack and does not exit from it because of the lower sheets of
239 insulation and wood.



240

241 **Figure 7 - Setup of the 2 cm water head exposure**

242 **5. Results and discussion**

243 **5.1. Morphology of healed cracks**

244 Concerning the visual observation of the panoramas, several aspects can be studied in addition to the crack geometry
245 parameters, such as the formation of precipitates inside the crack under different conditions.

246 As a first and most immediate aspect of the occurred crack sealing, it is worth noticing the whitish formations in control
247 and CA specimens when immersed in water, which can be clearly seen in Figure 8. For specimens conditioned in the
248 “water contact” environment, those white precipitates were only formed on the top face of the specimens, *i.e.*, on the face
249 in direct contact with water. This fact indicates that the transportation of water through the crack with a water head of 2
250 cm is not enough for ensuring healing of both faces, *i.e.* a complete healing throughout the thickness of the specimen.
251 However, despite the smaller reaction of the bottom crack, specimens stored in WC exposure got fairly good results
252 according to the healing rate achieved.

253 The formations were located all along the surface of the specimens in contact with water (for WI and WC exposures), not
254 only inside the crack, and were frequently accumulated also in some pores. In some cases, the precipitates were slightly
255 yellowish, which is supposed to be originated by the oxidation of steel fibers.

256 Another interesting aspect that could be studied through the analysis of the complete crack pattern panoramas is
257 determining whether the healing occurred only when the crack was in the cement paste or if it also occurred when the
258 crack broke through an aggregate or in the paste-aggregate interface. In the specimens with sealed or almost sealed
259 cracks this aspect was analyzed, and it was concluded that most formations were originated in the cement paste: this is
260 logical, because crystalline admixture is dispersed in concrete matrix among with the cement particles. Anyway, it was

261 also powerful enough to transport the healing products inside small cracked aggregates, which is an indicator of the
 262 effectiveness of the self-healing agent.

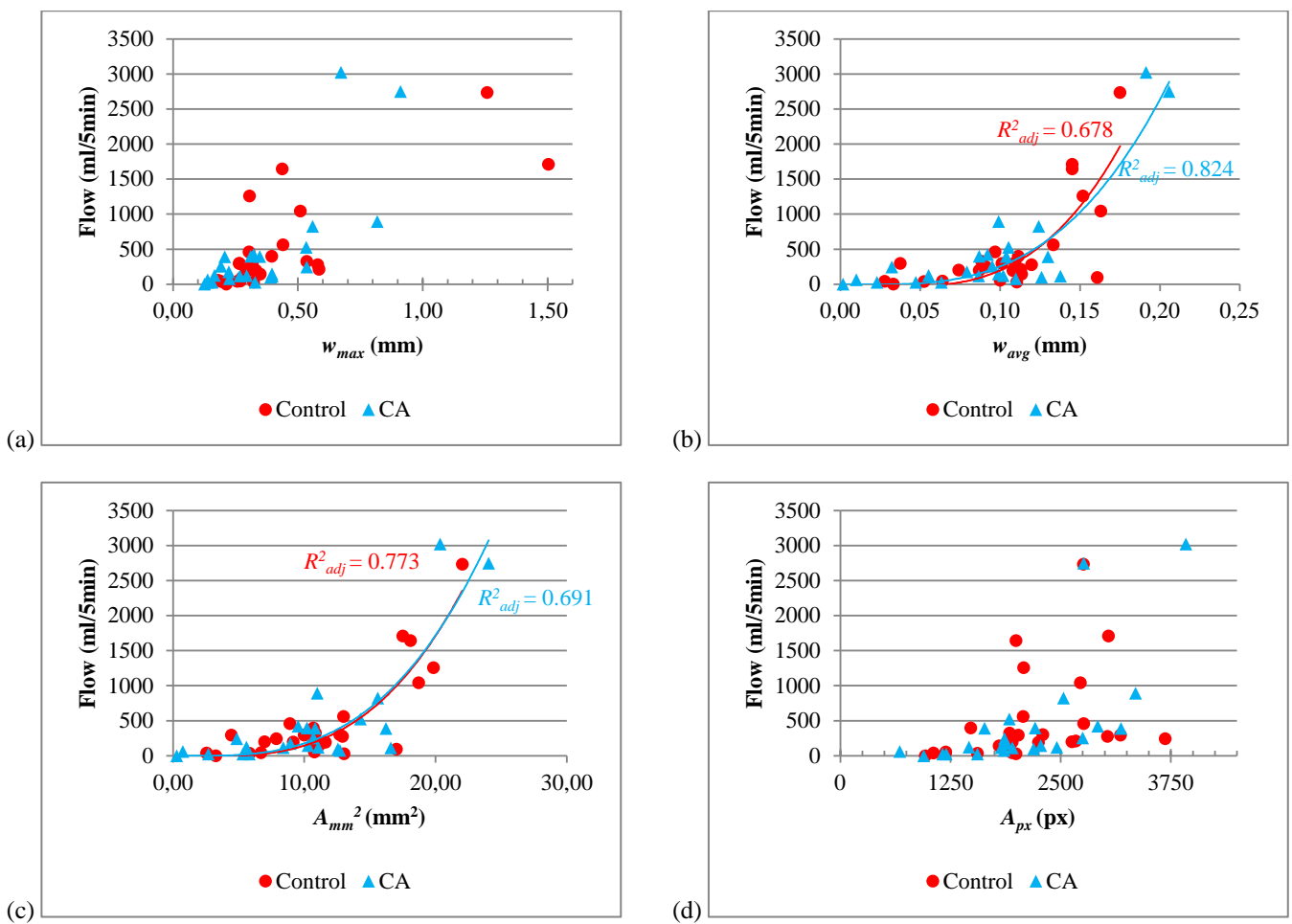
		Control concrete		Concrete with Crystalline Admixtures	
		Before healing	After healing	Before healing	After healing
EXPOSURE	Water Immersion		→		→
	Water Contact		→		→
	Humidity Chamber		→		→
	Air Exposure		→		→

263 **Figure 8 - Comparison between crack aspect at 0 days and after 42 days of healing, for control and CA specimens**
 264 **exposed to the four environments: water immersion (WI), water contact (WC), humidity chamber (HC) and air**
 265 **exposure (AE).**

266 **5.2. Self-healing results: water flow vs. crack geometry parameters**

267 When representing water flow versus the four crack geometry parameters obtained from image analysis of crack pattern
 268 panoramas (as detailed in section 4.3), it has to be observed that the best correlations were obtained from the relation
 269 between water flow and the A_{mm}^2 (Figure 9c) and with the averaged crack width w_{avg} (Figure 9a). The chosen trend lines
 270 are cubic functions depending on the crack geometry parameter: as explained from the literature, the water flow in a
 271 cracked specimen depends on the cube power of the crack width [7]. On the other hand, the correlation between water

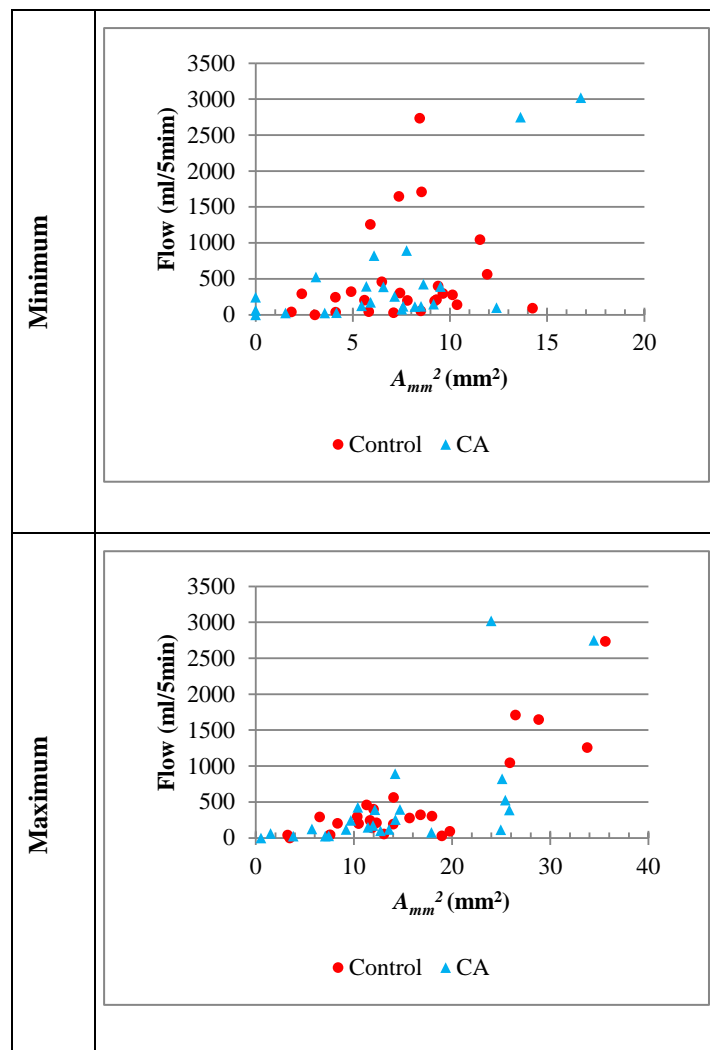
272 flow and w_{max} (Figure 9a) and A_{px} (Figure 9d) were highly dispersed and therefore these crack geometry parameters are
 273 proved to be worse indicators of the level of damage of the cracked specimens and the resulting self-healing.
 274 As a matter of fact, it can be observed that the measure of black pixels proved the worst one. There are two possible
 275 reasons for this behavior: a) the three-dimensional effect of the interior part of cracks, which makes crack pixels turn grey
 276 in the photographs while still being part of the crack; and b) the small interferences of black pixels outside the crack,
 277 though they were cleaned for minimizing this effect.
 278 For the two best methods, polynomial cubic trend lines were calculated by applying the boundary conditions of zero flow
 279 in correspondence of zero damage and horizontal tangent at zero flow. Adjusted R-squared (R^2_{adj}) was used in order to
 280 evaluate the goodness of fit of the model.

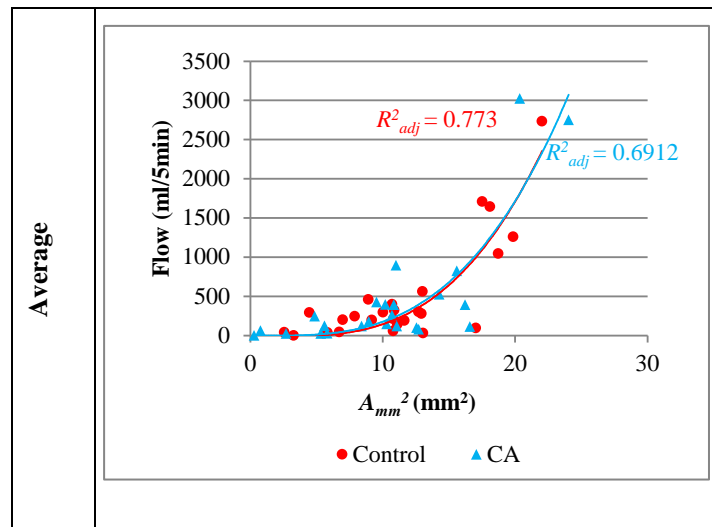


281 **Figure 9 - Relation between water flow and the geometrical parameters: (a) maximum crack width w_{max} , (b)**
 282 **averaged crack width w_{avg} , (c) estimated crack area A_{mm^2} , (d) amount of black pixels A_{px}**

283 It is important to remark that in each specimen two cracks were formed, on the top and the bottom surface. When
 284 choosing the value of the crack geometry parameter in order to study its relation with water flow, several options could
 285 be considered: the value of the parameter for the top/bottom crack, the minimum or the maximum, the average value, etc.

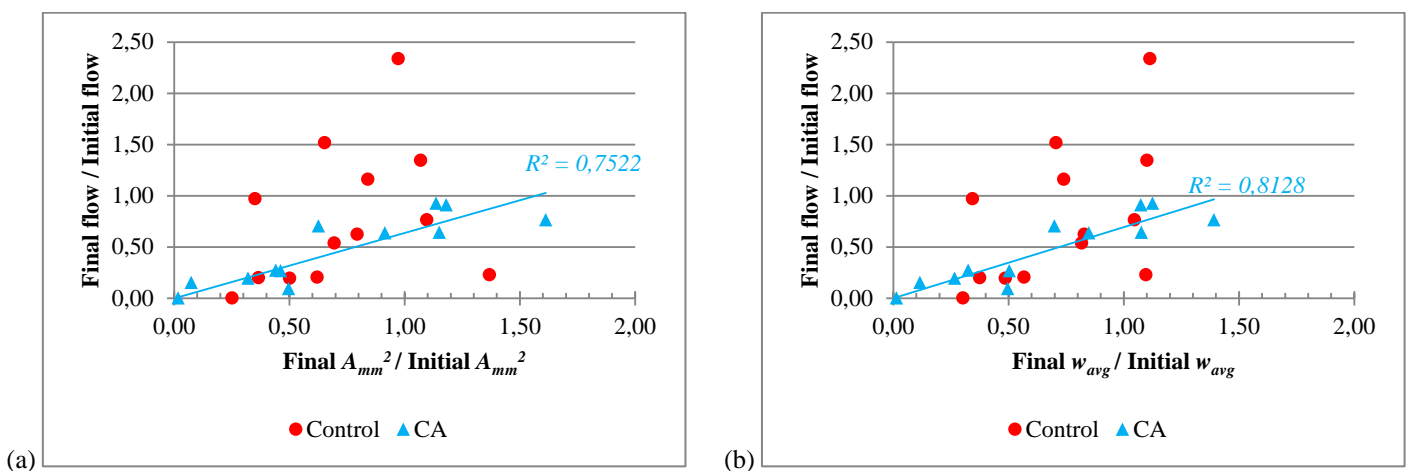
286 The minimum crack and the averaged crack were expected to be the best parameters in order to represent the damage
 287 comparing with the permeability results, the first option because the minimum section may restrict water flow and the
 288 latter because it is an estimation of the 3D volume of the crack considering it as a pyramidal frustum. The results in
 289 Figure 9 were represented using the averaged result from both top and bottom surface cracks. Other relations were also
 290 analyzed and they showed notably worse results, as it can be seen in Figure 10 for the cases of choosing the minimum,
 291 maximum and averaged value of cracks, for one of the best parameters, A_{mm}^2 . Choosing the top or the bottom crack as
 292 parameter did not showed any stable trend. Very similar results were achieved when analyzing the averaged crack width
 293 parameter w_{avg} . Thus, it can be assumed from the results in Figure 10 show that the averaged crack geometry parameter is
 294 the parameter that performs better.





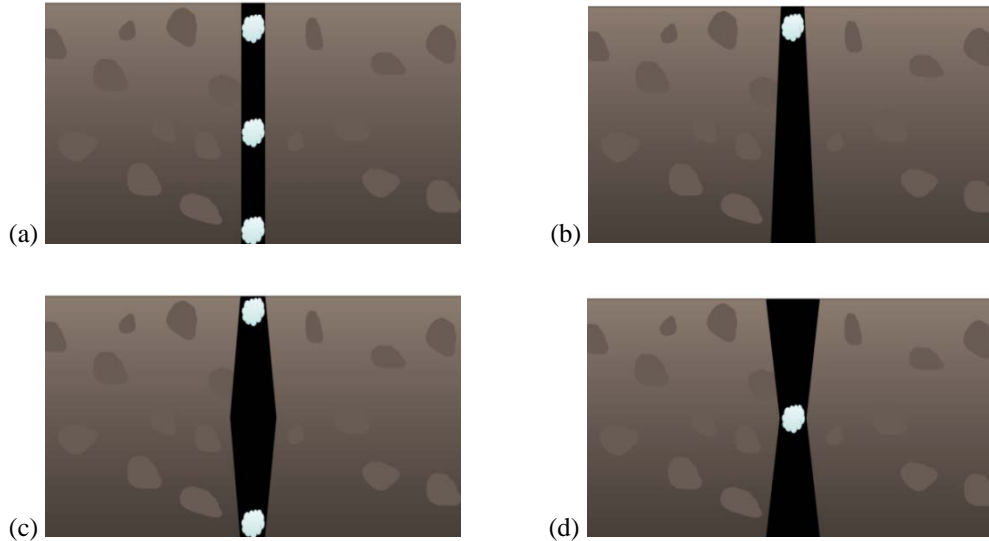
295 **Figure 10 - Initial water flow versus minimum, maximum and averaged estimated crack area A_{mm}^2**

296 The results of the relationship between the obtained ratios of final and initial water flow and the ratios from the final and
 297 initial values of the crack geometry parameters (averaged from the top and bottom cracks for each specimen) can be seen
 298 in the graphs in Figure 11. As expected higher water flow ratios correspond to higher crack geometry parameter ratios.
 299 Control specimens got significantly high dispersion while CA group showed a highly linear behavior for both
 300 methodologies of evaluating the crack geometry.



301 **Figure 11 - Relation between water flowratio and estimated crack area A_{mm}^2 ratio (a) and water flow ratio and**
 302 **averaged crack width w_{avg} ratio (b)**

303 The dispersion obtained in the results of this research could be caused by healing in different points of the interior of the
 304 crack since crystallization could start easily in the zones with lower crack width. Figure 12 represents a simplification of
 305 some of the possible interior morphologies of a crack in a concrete specimen, and the points that might be more suitable
 306 in order to start the precipitation of crack healing products. If the morphology of the crack is a concave volume, the
 307 interior of the crack may be healing while the visible crack would stay immutable, which could distort the calculated
 308 ratios and affecting the results.



309 **Figure 12 - Simplification of different possibilities for crack geometry in depth: uniform crack, pyramidal**
 310 **frustum, convex and concave forms and their most feasible points for precipitates**

311 In few words, comparing the previous results of the crack geometry parameters obtained from image analysis of crack
 312 pattern panoramas, it can be said that the measurements that most closely reflect the self-healing as evaluated by means
 313 of permeability recovery are the measure of crack area, averaged from crack width measured at different locations, (A_{mm}^2)
 314 and the averaged crack width (w_{avg}), as they minimize the dispersion. The dispersion in the correlation relationships
 315 between the healing ratio by permeability and healing ratio by crack geometry parameters could be caused by self-
 316 healing taking place inside a crack but not on the surface of the specimen, where the crack geometry parameters are
 317 measured.

318 5.3. Self-healing results: permeability

319 The self-healing properties based in the evolution of permeability are evaluated by means of the healing rate, which is
 320 defined as:

$$Healing\ Rate = 1 - \frac{Final\ Flow}{Initial\ Flow} = 1 - \frac{Q_{42}}{Q_0}$$

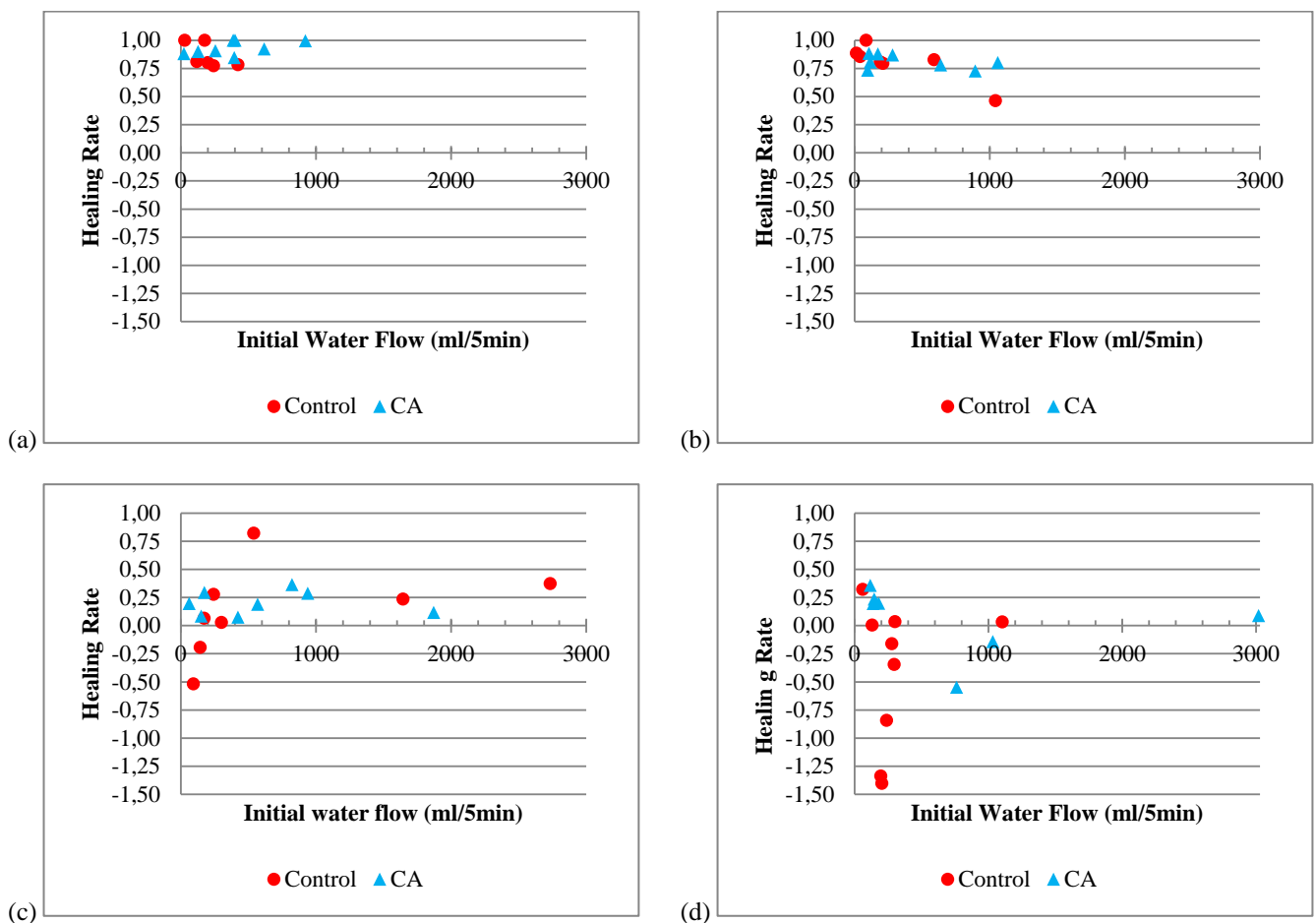
321 With:

322 Q_0 the initial water flow

323 Q_{42} the final water flow for a healing time of 42 days

324 When the final flow is similar to the initial flow, the healing rate would tend to 0; and when the final flow is 0, the
 325 healing rate would be 1. Negative values of the healing rate would show a reopening of the crack. The healing produced
 326 depending on the initial level of damage can be analyzed by representing the healing rates obtained for each specimen
 327 versus its initial water flow.

328 The specimens immersed in water (Figure 13a) and in contact with 2 cm of water layer (WC, Figure 13b) achieved
 329 higher healing rates. The exposure which showed the best healing behavior was water immersion, in which crystalline
 330 admixture specimens showed slightly better behavior than the control group. The importance of the presence of water for
 331 the self-healing reactions is proved. Nevertheless, the specimens stored in humidity chamber (Figure 13c) and in
 332 laboratory conditions (Figure 13d) showed lower results, with healing rate values generally lower than 0.5. It is worth
 333 noting that a more stable self-healing rate was achieved for specimens made with concrete containing the crystalline
 334 admixture (CA) than for control specimens, which show high dispersion as the amount of available water is reduced.



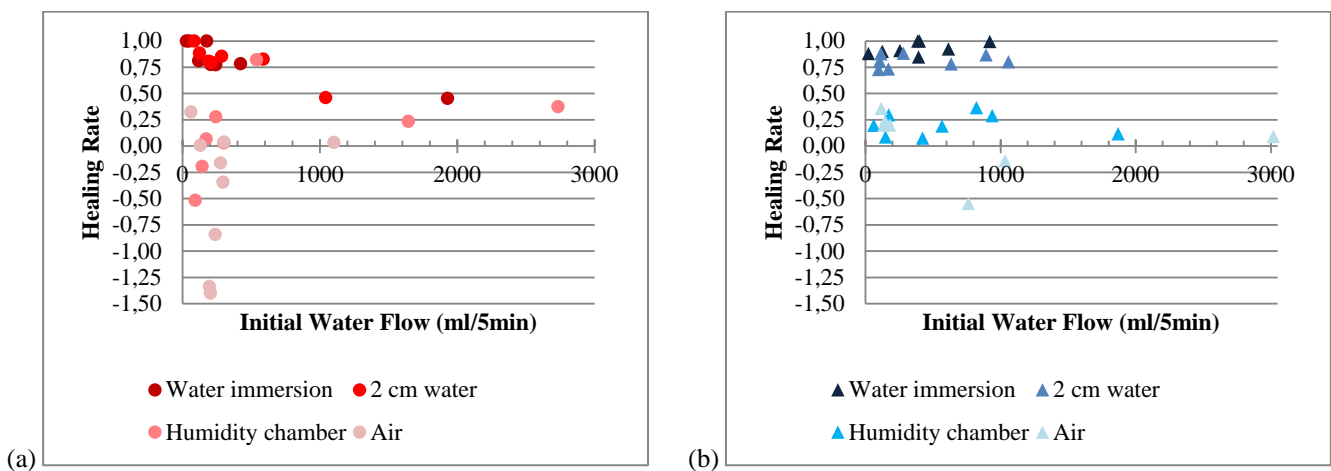
335 **Figure 13 - Control and CA concrete in the four exposures: water immersion (a), water contact (b), humidity**
 336 **chamber (c) and air exposure (d)**

337 In detail, specimens immersed in water showed values of healing rate between 0.75 and 1, those from the CA group
 338 showing higher values. For specimens in WC exposure there is a clear overlapping between the control and CA groups.
 339 In the HC group, control specimens showed higher dispersion, even reaching negative values of healing rate. It should be
 340 noted that in the group of laboratory exposure conditions, AE, there are several specimens with negative healing rates as
 341 well. This particular behavior can be caused by shrinkage, as specimens are young and the exposure has not enough
 342 humidity to compensate for the water loss, making the crack width even larger.

343 The same results, but classified depending on the type of mixture, are shown in Figure 14a (for control concrete) and
 344 Figure 14b (for CA concrete).

345 In the case of control specimens (Figure 14a), the results show a high dispersion. However, a clear tendency of better
 346 healing rates when increasing the available water can be observed. Moreover, no notable differences were observed
 347 between the specimens immersed in water immersion and those in water contact conditions.

348 On the other hand, for CA concrete (Figure 14b), the results can be clearly gathered in two groups: those in direct contact
 349 with water, either immersed or with a moderate head pressure, and those exposed to air humidity, either controlled or
 350 natural. Again, the more water available for the specimen, the higher healing rate is achieved. In the case of crystalline
 351 admixtures concrete, the results are clearly concentrated around the values of 0.93 for WI, 0.81 for WC; 0.21 for HC and
 352 0.17 for AE. This remarks the need of direct contact with water for the self-healing reactions to occur.



353 **Figure 14 - Behaviour of control concrete (a) and CA concrete (b) for the four different exposures**

354 Averaging the results of healing rates for the specimens with an initial water flow lower than 1000 milliliters per 5
 355 minutes (Figure 15), it can be clearly seen that the groups with higher healing rates are the groups with direct contact
 356 with water (WI and WC). In contrast, the specimens in humidity chamber showed a slightly better result with CA than
 357 for control concrete, but there is a significant difference with the previous groups. It can be hence argued that natural
 358 environmental humidity is not enough for complete self-healing to take place, even when using CA. However, it should
 359 be noted that when exposed to an environment with a lower humidity there is a big difference between the specimens
 360 made with concrete containing the crystalline admixture and the control concrete specimens. This is most likely due to
 361 drying shrinkage: in humidity chamber (HC) the water loss would be compensated, but not in the laboratory conditions
 362 (AE). In this case, the CA would act as a shrinkage compensator and the cracks, even if not healed, would at least be kept
 363 from growing.

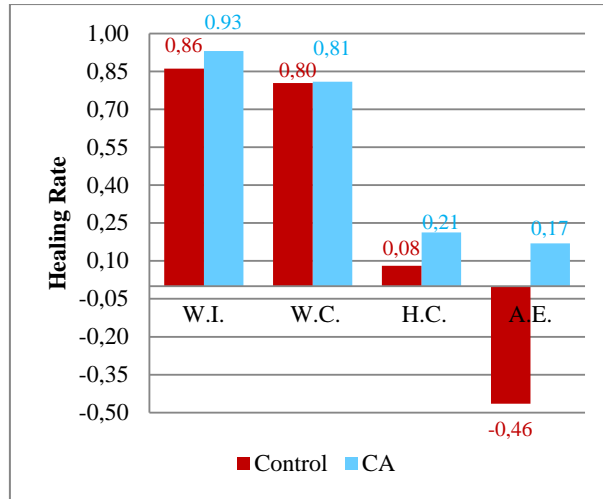


Figure 15 - Averaged Healing Rate for each group

364

365

366 5.4. Discussion

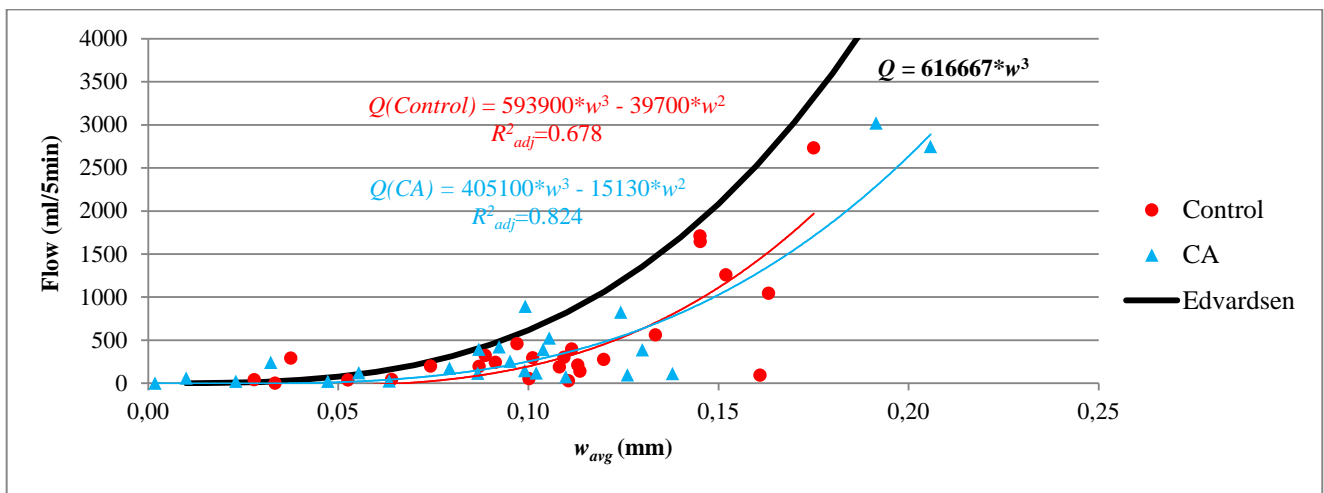
367 Edvardsen proposed a model based on Poiseuille Law [4], which is expressed in equation (1), for water at 20°C, viscosity
 368 $\nu = \eta/\rho = 1.00 \text{ mm}^2/\text{s}$ and a visible crack length of 1 meter; where q_0 is the water flow per meter length of crack, I is the
 369 hydraulic gradient in meters of water head per meter, w_{avg} is the mean value of crack width and k_t is a correcting
 370 parameter for temperature.

$$371 \quad q_0 \left(\frac{\text{liters}}{\text{m}} \right) = 740 * I * w_{avg}^3 * k_t \quad (1)$$

372 This expression can be adjusted to the parameters of the present research by changing units and the length of the crack
 373 (considered as 75 mm), resulting in the expression (2).

$$374 \quad Q \text{ (liters)} = 740 * \frac{20}{0.15} * w_{avg}^3 * 1 * 0.075 \quad (2)$$

375 The obtained experimental results of water flow and averaged crack width in this research (shown previously in Figure 9)
 376 fit reasonably well in the theoretical predictions given by equation (2) as displayed in Figure 16. The lower values
 377 obtained in this research might be due to the presence of fibers which could help blocking water flow inside the crack.



378

379 **Figure 16 - Comparison between experimental and theoretical water flow and crack width results**

380 With reference to the healing rates, similar values have been registered by other authors for permeability properties [16],
381 mechanical parameters or [19][20] closure of crack width [16][18] for specimens under water immersion exposure, with
382 values of effectiveness usually around 90% of recovery, or even higher. The enhancement of effectiveness by crystalline
383 admixtures specimens under water immersion comparing with results of control specimens has been also confirmed by
384 other studies [19], with results similar to those obtained in this work, increasing the healing capability about 7-10% with
385 respect to control concrete. The higher results of specimens from both groups (control and CA) under water immersion
386 WI compared to indoor or air exposure AE specimens obtained in this work are similar to those obtained studying the
387 recovery of mechanical properties in other studies [20].

388 **6. Conclusions**

389 This paper has presented the results of a research comparing different methodologies for quantifying the self-healing
390 capacity of fiber reinforced concrete and the effectiveness of crystalline admixtures as self-healing agent in four different
391 environmental exposures.

392 The following conclusions can be drawn from the obtained results:

393 With reference to the test methodology and to the parameters adopted to define and quantify the healing process rate:

- 394 1. Self-Healing Rate, calculated from the results of the modified permeability test designed in this research, is
395 a reliable indicator of the recovery of durability properties. The evaluation of permeability is, as a whole,
396 the best methodology in order to evaluate the damage in a concrete specimen.
- 397 2. The crack geometry parameters evaluated through image analysis have a clear relation with the water flow
398 results when comparing flow with the averaged crack area or the averaged crack width. This indicates that
399 the two aforementioned crack geometry parameters can be considered as alternative to water permeability
400 measurement tests. However, when correlating flow rates and crack geometry parameters in order to
401 evaluate the outcomes of self-healing processes, the dispersion is always higher for control specimens.
- 402 3. Still with reference to crack geometry parameters, the quantification of crack area through measurement of
403 black pixels of a crack panorama was the method which resulted in the highest dispersion of the values,
404 probably because of the three-dimensional effect of the depth of the cracks.

405 With reference to the influence of concrete composition and exposure conditions:

- 406 4. Self-healing process has been confirmed for both cases: autogenous healing of control concrete and healing
407 caused by crystalline admixtures reactions.

- 408 5. Specimens cast with concrete containing crystalline admixtures and stored under water immersion achieved
409 the highest self-healing rates, with values around 95% even for the larger initial crack width.
410 Specimens with crystalline admixtures showed a more stable and reliable behavior in healing tests showing
411 lower dispersion and clearer trends.
- 412 6. The presence of water is critical for the self-healing to take place for both reference concrete and crystalline
413 admixture concrete, leading to self-healing rates above 80-90% respectively. The two exposures with direct
414 contact of water had significantly higher healing rates than those under different values of air humidity,
415 confirming the need of water for the reaction.
- 416 7. The presence of a layer of 2 cm of water in one crack is enough to make the self-healing rate to increase to
417 levels of 80%, with low differences between both types of concrete.

418 **Acknowledgements**

419 The authors would like to thank Sika AG and Elite Cementos S.L. for the material donations for the project.

420 **References**

- 421 [1] Wua M, Johannesson B, Geiker M. A review: Self-healing in cementitious materials and engineered
422 cementitious composite as a self-healing material. *Construction and Building Materials* 2012; 28:571–583
- 423 [2] Neville AM. *Properties of Concrete*, Third Edition, Longman, 1981, 779pp.
- 424 [3] Hearn N. Self-sealing, autogenous healing and continued hydration: What is the difference? *Materials and*
425 *Structures/Matériaux et Constructions* 1998; 31:563-567
- 426 [4] Edvardsen C. Water Permeability and Autogenous Healing of Cracks in Concrete. *ACI Materials Journal* 1999,
427 July-August:448-454
- 428 [5] Ter Heide N. Crack healing in hydrating concrete. MSc-thesis, Delft University of Technology Faculty of Civil
429 Engineering and Geosciences 2005, 128pp
- 430 [6] Van Tittelboom K, Gruyaert E, Rahier H, De Belie N. Influence of mix composition on the extent of autogenous
431 crack healing by continued hydration or calcium carbonate formation. *Construction and Building Materials*
432 2012; 37: 349–359
- 433 [7] Qian S, Zhou J, de Rooij MR, Schlangen E, Yea G, van Breugel K. Self-healing behavior of strain hardening
434 cementitious composites incorporating local waste materials. *Cement & Concrete Composites* 2009; 31:613–621
- 435 [8] Zhang Z, Qian S, Ma H. Investigating mechanical properties and self-healing behavior of micro-cracked ECC
436 with different volume of fly ash. *Construction and Building Materials* 2014; 52:17–23

- 437 [9] Qian SZ, Zhou J, Schlangen E. Influence of curing condition and precracking time on the self-healing behavior
438 of Engineered Cementitious Composites. *Cement & Concrete Composites* 2010; 32:686-693
- 439 [10] Nishiwaki T, Kwon S, Homma D, Yamada M, Mihashi H. Self-Healing Capability of Fiber-Reinforced
440 Cementitious Composites for Recovery of Watertightness and Mechanical Properties. *Materials* 2014; 7:2141-
441 2154
- 442 [11] Nishiwaki T, Koda M, Yamada M, Mihashi H, Kikuta T. Experimental Study on Self-Healing Capability of
443 FRCC Using Different Types of Synthetic Fibers. *Journal of Advanced Concrete Technology* 2012; 10:195-206
- 444 [12] Yang Y, Yang EH, Li VC. Autogenous healing of engineered cementitious composites at early age. *Cement and*
445 *Concrete Research* 2011; 41:176-183
- 446 [13] Perez G, Jimenez I, Erkizia E, Gaitero JJ, Kaltzakorta I, Guerrero A. Effect of self-healing additions on the
447 development of mechanical strength of cement paste. *Chemistry and Materials Research* 2013; 5:102-105
- 448 [14] Yang Z, Hollar J, He X, Shi X. A self-healing cementitious composite using oil core/silica gel shell
449 microcapsules. *Cement & Concrete Composites* 2011; 33:506-512
- 450 [15] Jonkers HM, Schlangen E. Crack repair by concrete-immobilized bacteria. *Proceedings of the First International*
451 *Conference on Self Healing Materials*, 18-20 April 2007, Noordwijk aan Zee, The Netherlands
- 452 [16] Sisomphon K, Copuroglu O, Koenders EAB. Self-healing of surface cracks in mortars with expansive additive
453 and crystalline additive, *Cement & Concrete Composites* 2012; 34:566-574
- 454 [17] ACI Committee 212, 2010. Report ACI 212-3R-10, 2010. Report on chemical admixtures for concrete.
455 American Concrete Institute (ACI), Chapter 15, pp 46-50
- 456 [18] Jaroenratanapirom D, Sahamitmongkol R. Self-Crack Closing Ability of Mortar with Different Additives,
457 *Journal of Metals, Materials and Minerals* 2011; 21: 9-17
- 458 [19] Ferrara L, Krelani V, Carsana M. A “fracture testing” based approach to assess crack healing of concrete with
459 and without crystalline admixtures, *Construction and Building Materials* 2014; 68:535-551
- 460 [20] Sisomphon K, Copuroglu O, Koenders EAB. Effect of exposure conditions on self healing behavior of strain
461 hardening cementitious composites incorporating various cementitious materials. *Construction and Building*
462 *Materials* 2013; 42:217-224
- 463 [21] Desmettre C, Charron J-P. Novel water permeability device for reinforced concrete under load, *Materials and*
464 *Structures* 2011; 44:1713-1723